Cell. Mol. Biol. (ISSN: 1165-158X)

Journal Homepage: www.cellmolbiol.org

Cellular and Molecular Biology

Original Research Article

Autotaxin as a potential biomarker in hepatic encephalopathy: Insights from a mouse model and cirrhotic patients

Ali Sepehrinezhad[1,2], Hossein Zarei[1], Farhad Mehravaran[3], Sepehr Sadr[3], Meysam Heydar Ahmad[3], Fariborz Rezaeitalab[4], Mahshid Mahyad[4], Vahid Hajali[5], Ali Shahbazi[6,7*], Ali Beheshti Namdar[8*], Sajad Sahab Negah[9*]

[1] *Neuroscience Research Center, Mashhad University of Medical Sciences, Mashhad, Iran*
[2] *Department of Neuroscience, Faculty of Medicine, Mashhad University of Medical Sciences, Mashhad, Iran*
[3] *Faculty of Medicine, Mashhad University of Medical Sciences, Mashhad, Iran*
[4] *Department of Neurology, Faculty of Medicine, Mashhad University of Medical Sciences, Mashhad, Iran*
[5] *Quchan School of Nursing, Mashhad University of Medical Sciences, Mashhad, Iran.*
[6] *Cellular and Molecular Research Center, Iran University of Medical Sciences, Tehran, Iran*
[7] *Department of Neuroscience, Faculty of Advanced Technologies in Medicine, Iran University of Medical Sciences, Tehran, Iran*
[8] *Department of Internal Medicine, Faculty of Medicine, Mashhad University of Medical Sciences, Mashhad, Iran*
[9] *Multiple Sclerosis Research Center, Neuroscience Institute, Tehran University of Medical Sciences, Tehran, Iran*

Article Info

Article history:

Received: March 13, 2026
Accepted: May 16, 2026
Published: May 31, 2026

Use your device to scan and read the article online

Abstract

Hepatic encephalopathy (HE) is a debilitating neuropsychiatric condition associated with acute liver failure or advanced liver diseases, significantly affecting patient morbidity and mortality. Autotaxin (ATX), a lysophospholipase D that generates lysophosphatidic acid (LPA), has been proposed as a biomarker for liver fibrosis progression, but its role in HE remains poorly defined. This study aimed to explore the potential roles of ATX using in vivo TAA-induced HE models in mouse and clinical evaluations of cirrhotic patients with and without HE. ATX concentrations were quantified in plasma, liver tissue, and frontal cortex of HE mice, while ectonucleotide pyrophosphatase/phosphodiesterase 2 (Enpp2) gene expression and LPA levels were assessed in murine salivary glands. In parallel, serum and salivary ATX were measured in 7 cirrhotic patients with HE and 12 cirrhotic patients without HE. ATX concentrations were significantly elevated in the liver parenchyma and frontal cortex of TAA-induced HE mice compared to controls, whereas plasma ATX showed no significant difference. Enpp2 expression was upregulated 2.49-fold in salivary glands of HE mice, although salivary LPA concentrations did not differ between groups. Clinically, both serum and salivary ATX levels were significantly higher in cirrhotic patients with HE than in those without HE. Moreover, salivary ATX levels positively correlated with serum alkaline phosphatase (ALP) levels in the HE patient group. These findings demonstrate that ATX is elevated in key tissues and biofluids in both experimental and clinical HE, supporting its potential as a novel biomarker. Moreover, the data suggest that the ATX-LPA axis may contribute to HE pathophysiology, providing a foundation for future mechanistic studies and the exploration of targeted therapeutic strategies.

Keywords: Hepatic encephalopathy; Autotaxin; Serum; Saliva; Cirrhosis; Patients; Thioacetamide; Mice; Brain; Liver

1. Introduction

Hepatic encephalopathy (HE) represents a complex neuropsychiatric complication arising from acute liver failure or chronic liver disease, significantly impacting patient outcomes and quality of life [1, 2]. The HE pathophysiology is multifactorial; hence, many biochemical and neuroinflammatory processes that interfere with normal brain functioning are part of it. It has traditionally been thought that the accumulation of ammonia was the most critical factor in HE pathogenesis [3, 4]. More recent studies have suggested that autotaxin (ATX) could be a promising biomarker for chronic liver disease progression and acute-on-chronic liver failure [5-9]. ATX, coded by ectonucleotide pyrophosphatase/phosphodiesterase 2 (ENPP2) gene, is a secreted lysophospholipase D that synthesizes lysophosphatidic acid (LPA) from lysophosphatidylcholine and maintains the primary source of circulating LPA [10, 11]. LPA, the enzymatic product of ATX, is a bioactive lipid mediator that modulates diverse cellular processes including inflammation, angiogenesis, fibrosis, and vascular permeability through six G-protein-coupled receptors (LPAR1-6) [12-14].

Elevated levels of ATX have been correlated with tissue inflammation and fibrosis of liver parenchyma in patients with non-alcoholic fatty liver disease (NAFLD), chronic hepatitis B, and primary biliary cholangitis [5, 6,

* Corresponding author.
E-mail address: shahbazi.a@iums.ac.ir (A. Shahbazi); Beheshtia@mums.ac.ir (A. B. Namdar); (S. S. Negah) sahabsajad@yahoo.com.
Doi: http://dx.doi.org/10.14715/cmb/2026.72.5.2

8, 15, 16]. Moreover, serum ATX concentrations correlated well with liver function parameters and the Model for End-Stage Liver Disease (MELD) score in patients with chronic hepatitis B [9]. Furthermore, preclinical animal studies have demonstrated the role of the ATX-LPA axis in the pathogenesis of acute liver failure, NAFLD, non-alcoholic steatohepatitis, and cirrhosis [8, 17, 18]. We also previously confirmed elevated plasma and cerebral LPA levels in thioacetamide (TAA)-induced HE mice [19].

Current treatment strategies to ameliorate HE mainly concentrate on reducing the ammonia level by dietary modification. While these approaches have proven effective in many cases, they do not clinically reduce the underlying inflammatory and neuroinflammatory processes [20-22]. While ATX is established in liver fibrosis, its specific role in HE, particularly regarding central nervous system (CNS) effects, remains unexplored. This study aimed to investigate the role of the ATX-LPA axis in the progression of HE by measuring ATX concentrations in several biological samples (plasma, liver tissues, and cerebral cortex) of HE mice, as well as serum and saliva from patients with liver cirrhosis with or without HE. By comparing the levels of ATX in the saliva and serum of patients with laboratory parameters, we seek to elucidate the relationship between this biomarker and the severity of the disease.

2. Materials and Methods

2.1. Ethical statement

In this study, all experimental animal procedures were conducted following ARRIVE guidelines and were approved by the Ethical Committee of Animal Care at Iran University of Medical Sciences, Tehran, Iran, 2020 (IR.IUMS.REC.1398.959). The clinical section of the study received approval from the Institutional Review Board Ethics Committee of Mashhad University of Medical Sciences, Mashhad, Iran, 2022 (IR.MUMS.MEDICAL.REC.1401.141), and the protocol conforms to the provisions of the Declaration of Helsinki. Furthermore, informed consent was obtained from all patients or their legal guardians.

2.2. Mouse model of HE and study groups

Male C57BL/6 mice, aged 10 to 12 weeks and weighing between 25 and 30 grams, were obtained from the Animal Center of Iran University of Medical Sciences. The mice were kept in a controlled environment with a temperature of 23 ± 2°C and relative humidity of 50-60%, under a 12-hour light/dark cycle and provided unrestricted access to rodent chow and water in bottles. HE was induced using two consecutive intraperitoneal injections of TAA (Sigma-Aldrich, USA) at 600 $mg.kg^{-1}$, administered with a 24-hour interval in normal saline. The TAA dose and dosing interval were selected based on our previous study, in which this established protocol reliably induced HE with reproducible clinical and biochemical features while avoiding excessive mortality [19]. The HE phenotype was confirmed based on established neurological and biochemical criteria, and the severity of HE was graded according to the criteria described in our previous studies [19, 23]. The animals had continuous access to food and wet pellets on the cage floor. A daily maintenance solution of dextrose in normal saline was administered subcutaneously to prevent hypoglycemia and dehydration. Control-vehicle mice received only intraperitoneal injection of normal saline as solvent of TAA for two consecutive days.

2.3. Measurement of ATX and LPA

The levels of ATX in plasma, liver tissues, and the cerebral cortex of mice, as well as in serum and saliva samples from patients, were quantified according to specific sandwich enzyme-linked immunosorbent assay (ELISA) kits. This was performed using a commercially available kit from ZellBio GmbH, Germany, according to the manufacturer's instructions. Pre-weighed tissues were homogenized in an ice-cold PBS solution and subsequently centrifuged. The supernatants were collected for further analysis. All samples were measured at 450 nm. A similar method was conducted to measure the levels of LPA in the salivary glands of HE mice.

2.4. RNA isolation, cDNA synthesis, and reverse transcription

Total RNA was isolated from the salivary glands of mice using an RNA extraction kit (Yektatajhiz Azma, Iran) following the manufacturer's guidelines. Complementary deoxyribonucleic acid (cDNA) was synthesized using a cDNA synthesis kit (Yektatajhiz Azma, Iran). Following this, reverse transcription-quantitative polymerase chain reaction (RT-qPCR) was conducted using the synthesized cDNA, along with gene-specific primers for Enpp2 (forward: TCCCTACCCACTACTACAGCATC; reverse: AGACACAGAGAGAGGACCATCAC; Pishgam Biotech Co, Iran) and SYBR Green qPCR reagents (Yektatajhiz Azma, Iran) on a LightCycler 96 (Roche, Switzerland). This was performed using the following cycling conditions: preincubation at 95°C for 900 seconds, two-step amplification by 40 cycles of 95°C for 30 seconds and 60°C for 60 seconds and melting. Gene expression levels were normalized to the reference gene glyceraldehyde 3-phosphate dehydrogenase (GAPDH; forward: CAACGACCCCTTCATTGACC; reverse: CTTCCCATTCTCGGCCTTGA; Pishgam Biotech Co, Iran), and relative gene expression was calculated using the $2^{-\Delta\Delta Ct}$ method. All results were demonstrated as relative fold changes compared to the control-vehicle group.

2.5. Patients

This case-control study was conducted from 2022 until May 2024. Patients were recruited from the Internal Medicine Department of Ghaem Hospital in Mashhad, Iran. The study received approval from the Mashhad University of Medical Sciences ethics committee, and all participants were given informed written consent. Nineteen participants were included in the study, consisting of seven cirrhotic patients with HE and twelve cirrhotic patients without HE, who were selected as the control group.

The severity of cirrhosis was evaluated using the Child-Pugh Score, MELD score, and MELD-Na score [24-26]. Also, the levels of aspartate aminotransferase (AST), alanine aminotransferase (ALT), alkaline phosphatase (ALP), total bilirubin, direct bilirubin, albumin, creatinine, urea, sodium, potassium, and c-reactive protein (CRP) were measured. Partial thromboplastin time (PTT) and international normalized ratio (INR) were also measured in all participants. Patients were monitored for the presence of ascites. Hematological parameters, including white blood cell (WBC) count, red blood cell (RBC) count, hemoglobin (Hb), hematocrit (HCT), platelet (PLT) count, percen-

tage of polymorphonuclear (PMN) cells, and percentage of lymphocytes, were also evaluated. The HE grade in cirrhotic patients with HE was determined according to the West Haven Criteria [27]. Patients with HE of West Haven grade III or IV were excluded from the study. Patients with other major neurological or psychiatric disorders, active infection, recent gastrointestinal bleeding, acute kidney injury, or other conditions that could independently affect neurological status or circulating biomarker levels were also excluded. Cirrhosis was confirmed based on clinical assessment and compatible imaging findings, including characteristic morphological changes of the liver and signs of portal hypertension; liver biopsy was not routinely performed.

2.6. Data analysis

All statistical analyses were conducted using GraphPad Prism version 9. The data are presented as mean ± standard error of the mean (SEM). Data were first tested for normality using the Shapiro-Wilk test. Normally distributed data were analyzed using parametric tests, whereas non-normally distributed data were analyzed using non-parametric tests. The Student's t-test was used for comparisons of quantitative variables between the two experimental groups for parametric data, while the Mann-Whitney U test was applied for non-parametric data. Pearson's correlation was used to evaluate linear relationships between normally distributed variables, whereas Spearman's correlation was used for non-parametric variables. A P value ≤0.05 was considered statistically significant.

2.7. Identifying new related target proteins for the ATX-LPA axis and predicting upstream signaling pathways through a bioinformatics approach

We uploaded genes related to ATX-LPA axis to predict additional significant proteins associated with the axis, such as ENPP2, LPAR1, LPAR2, LPAR3, LPAR4, LPAR5, and LPAR6, into the STRING database. We analyzed selecting Homo sapiens as the organism. We predicted several novel proteins based on the protein-protein interaction data from this database. Also, we identified the most significant pathways related to the ATX-LPA axis and these associated novel proteins through KEGG pathways, Reactome pathways, and Wikipathways. For pathway enrichment analysis, pathways were considered significantly enriched when the adjusted P value (false discovery rate, FDR) was <0.05. Enrichment scores were interpreted as a measure of the over-representation of ATX-LPA axis-associated proteins within a given pathway relative to the expected proportion in the reference background; higher enrichment scores therefore indicated a stronger association between the identified proteins and the corresponding biological pathway. Multiple-testing correction was applied using the Benjamini-Hochberg method.

3. Results

3.1. ATX concentration, as well as ENPP2 and LPA expression in an animal model

The levels of plasma ATX were not statistically significant between HE mice and the control-vehicle group (117.6±3.273 vs. 134.7±7.481 ng.ml^{-1} in HE and control mice, respectively; Figure 1A). However, the expression of the ATX gene (ENPP2) in the salivary glands was significantly higher in HE mice compared to the control-vehicle group (2.491±0.4854 in HE vs. 1.00±0.0490 in control mice; Figure 1B). Additionally, in these tissues, the levels of LPA did not display a statistical difference between the animal groups (292.5±189.5 vs.112.7±55.36 umol.L-1 in HE and control-vehicle mice, respectively; Figure 1C). Furthermore, the levels of ATX in the liver parenchyma (195.2±21.87 vs. 128.8±12.56 ng.ml^{-1} in HE and control mice, respectively; Figure 1D) and frontal cortex (156.5±12.46 vs. 111.5±2.779 ng.ml^{-1} in HE and control mice respectively; Figure 1E) of TAA-induced HE mice were significantly increased compared to control-vehicle mice.

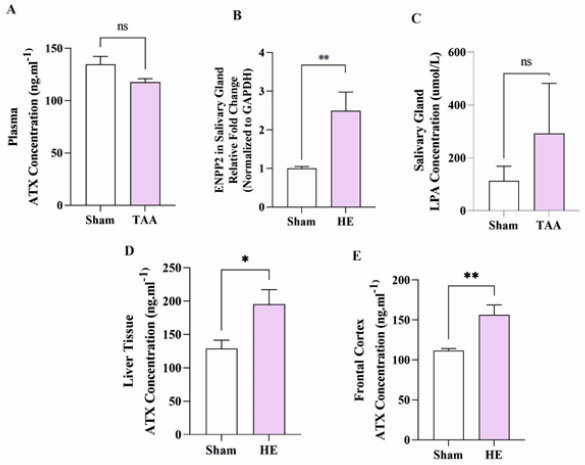


Fig. 1. Comparison of ATX levels, ENPP2 expression, and LPA levels between control-vehicle (sham) and HE mice. (A) Plasma levels of ATX (n = 5-7), (B) salivary ENPP2 expression (n = 4), (C) salivary LPA concentrations (n = 4-5), (D) liver ATX levels (n = 7) and (E) cerebral cortex ATX levels (n = 5-6) between sham and TAA-induced HE mice. Data are presented as mean ± SEM.

3.2. Baseline demographic and laboratory parameters of patients

As shown in Table 1, there was no statistically significant difference in age between the groups (61±3.71 vs. 63±4.51 years in cirrhotic-controls and cirrhotic-HE, respectively). However, the average blood urea levels were significantly higher in cirrhotic-HE compared to cirrhotic-controls (34.50±4.80 vs. 64.17±10.38 mg.dl^{-1} in cirrhotic-controls and cirrhotic-HE respectively; P< 0.01). HB levels were also statistically elevated in cirrhotic-HE compared to cirrhotic-controls (10.16±0.34 vs. 12.11±0.69 g.dl^{-1} in cirrhotic-controls and cirrhotic-HE, respectively; P< 0.05). Furthermore, the percentage of HCT was increased in cirrhotic-HE compared to cirrhotic-controls (32.24±0.91vs. 37.70±1.60 percent in cirrhotic-controls and cirrhotic-HE respectively; P< 0.01).

3.3. Baseline levels of ATX in serum and saliva between patient groups

According to the results of the ELISA assay, the concentration of ATX in serum was significantly increased in cirrhotic-HE patients compared to cirrhotic-control groups (199.9±32.42 vs. 380.5±79.88 ng.ml^{-1} in cirrhotic-controls and cirrhotic-HE respectively; P< 0.05; Figure 2A). Similarly, the average levels of ATX in saliva were significantly increased in cirrhotic-HE patients compared to cirrhotic-control groups (220.1±28.09 vs. 516.7±162.5

Table 1. Serum biochemistry and hematological parameters of cases.

Parameters	Cirrhotic-control (n=12)	Cirrhotic-HE (n=7)	P value
Gender (M/F)	(7/5)	(5/2)	-
Age	61±3.71	63±4.51	0.7419
Urea ($mg.dl^{-1}$)	**34.50±4.80**	**64.17±10.38****	**0.0086**
Creatinine ($mg.dl^{-1}$)	1.164±0.14	1.346±0.26	0.5250
Sodium ($mEq.L^{-1}$)	137.5±1.13	135±5.56	0.5796
Potassium ($mEq.L^{-1}$)	3.82±0.20	4.18±0.32	0.3378
AST ($U.L^{-1}$)	76.08±18.05	115.7±36.08	0.2991
ALT ($U.L^{-1}$)	62.33±19.47	130±50.01	0.0556
ALP ($U.L^{-1}$)	289.6±32.93	398±62.11	0.1103
Total bilirubin ($mg.dl^{-1}$)	8.78±3.13	8.94±3.44	0.6956
Direct bilirubin ($mg.dl^{-1}$)	4.14±1.43	4.98±2.09	0.7357
WBC($*10^3.mcl^{-1}$)	9.63±2.51	6.84±1.35	0.4334
RBC($*10^6.mcl^{-1}$)	3.39±0.16	3.92±0.25	0.0824
HB ($g.dl^{-1}$)	**10.16±0.3**4	**12.11±0.69***	**0.0123**
HCT (%)	**32.24±0.91**	**37.70±1.60****	**0.0036**
MCV (fL)	94.94±2.49	93.74±1.77	0.7406
MCH (pg)	30.27±0.98	30.97±0.80	0.6318
MCHC ($g.dl^{-1}$)	31.84±0.41	33.02±0.38	0.0751
PLT($*10^3.mcL^{-1}$)	99.58±26.56	69±14.38	0.4175
PMN(%)	73.41±4.53	64.87±6.37	0.2816
Lymph(%)	19.97±3.34	18.92±2.91	0.8300
PTT (sec)	44.33±3.00	47.00±4.92	0.6291
INR	1.59±0.10	1.89±0.14	0.0956
Albumin ($g.dl^{-1}$)	2.71±0.10	2.24±0.35	0.1351
CRP ($mg.L^{-1}$)	39.34±12.61	39.41±10.15	0.9966
Ascites (N)	11	5	-
MELD score	18.36±1.49	21.77±2.70	0.2452
MELD-Na score	17.95±1.74	21.67±4.85	0.3988
Child-Pugh Score	10.00±0.26	11.43±0.75	0.0521
West Haven Criteria	-	1.42±0.20	-

Data are expressed as mean± SEM. * Compared to cirrhotic-control. *P < 0.05, and **P < 0.01

$ng.ml^{-1}$ in cirrhotic-controls and cirrhotic-HE respectively; P< 0.05; Figure 2B).

3.4. Correlation between saliva and serum ATX with laboratory parameters in cirrhotic-control and cirrhotic-HE patients

Correlation analysis indicated that saliva ATX levels were positively correlated with an essential marker of disease severity, ALP, in the cirrhotic-HE group (r = 0.87, P = 0.02; Table 2). There were no significant correlations between saliva ATX levels and other laboratory parameters in both the cirrhotic-control and cirrhotic HE groups (Table 2).

On the other hand, serum ATX levels were significantly correlated with blood urea levels (r = -0.62, P = 0.04) and PLT count (r = 0.61, P = 0.04) in the cirrhotic-control group (Table 3). In the Cirrhotic-HE group, the levels of serum ATX were positively correlated with blood MCH levels (r = 0.77, P = 0.04; Table 3). No significant correlations were found between serum levels of ATX and other laboratory parameters in the cirrhotic-control or cirrhotic HE groups (Table 3).

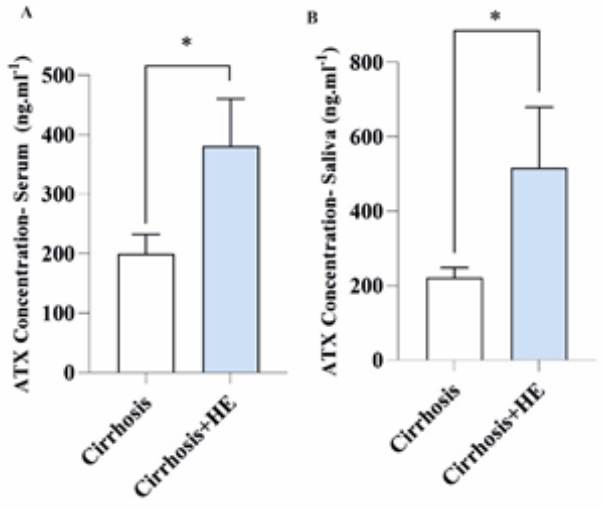


Fig. 2. Comparison of serum (A) and saliva (B) ATX levels between cirrhotic-control and cirrhotic-HE patients. Unpaired t-test analysis. Data are presented as mean ± SEM.

Table 2. Correlation between saliva ATX levels with laboratory parameters in cirrhotic-control and cirrhotic-HE groups.

Parameters	Saliva ATX			
	Cirrhotic-Control		Cirrhotic-HE	
	Correlation coefficient (r)	P value	Correlation coefficient (r)	P value
Urea	0.14	0.68	-0.51	0.3785
Creatinine	0.20	0.57	-0.54	0.2658
Sodium	-0.13	0.71	0.00	0.99
Potassium	0.06	0.85	-0.01	0.98
AST	0.00	>0.99	-0.14	0.80
ALT	-0.16	0.65	-0.11	0.83
ALP	0.31	0.37	**0.87**	**0.02**
Total bilirubin	0.26	0.46	-0.17	0.75
Direct bilirubin	0.15	0.67	-0.18	0.72
WBC	-0.34	0.33	-0.04	0.93
RBC	-0.55	0.09	-0.18	0.72
HB	-0.20	0.56	-0.06	0.90
HCT	-0.34	0.33	-0.06	0.89
MCV	0.40	0.24	0.35	0.48
MCH	0.44	0.20	0.28	0.58
MCHC	0.41	0.23	0.00	0.98
PLT	-0.41	0.23	0.05	0.91
PMN	-0.12	0.73	0.31	0.56
Lymph	0.01	0.97	-0.18	0.72
PTT	0.08	0.80	0.01	0.98
INR	0.04	0.89	-0.23	0.65
Albumin	-0.09	0.79	-0.02	0.98
CRP	-0.43	0.21	-0.45	0.36
MELD score	0.43	0.20	-0.64	0.17
MELD-Na score	0.41	0.23	-0.32	0.53
Child-Pugh Score	0.14	0.71	-0.11	0.82
West Haven Criteria	-	-	0.00	>0.99

3.5. Novel proteins and pathways associated with ATX-LPA axis

Based on protein-protein interaction data from STRING, we predicted five novel proteins associated with the ATX-LPA axis including glycerophosphodiester phosphodiesterase domain containing 1 (GDPD1), glycerophosphodiester phosphodiesterase domain containing 3 (GDPD3), cholinergic receptor muscarinic 1 (CHRM1), cholinergic receptor muscarinic 2 (CHRM2), and phosphoinositide 3-kinase regulatory subunit 6 (PIK3R6). The protein network analysis revealed 12 nodes and 57 edges, with an average node degree of 9.5 and an average local clustering coefficient of 0.918 (Figure 3A).

KEGG pathway analysis indicated that the most significantly enriched pathways related to the ATX-LPA axis included the PI3K-Akt signaling pathway, phospholipase D signaling pathway, neuroactive ligand-receptor interaction, regulation of the actin cytoskeleton, and the Rap1 signaling pathway (Figure 3B).

Reactome pathway enrichment analysis also highlighted several key pathways associated with the ATX-LPA axis, including Class A/1 (Rhodopsin-like receptors), GPCR downstream signaling, G alpha (q) signaling events, lysosphingolipid and LPA receptors, G alpha (i) signaling events, and muscarinic acetylcholine receptors (Figure 3C).

Furthermore, the results from Wikipathways enrichment revealed significant pathways such as the PI3K-Akt signaling pathway, focal adhesion: PI3K-Akt-mTOR signaling pathway, GPCRs, class A rhodopsin-like, nucleotide GPCRs, purinergic signaling, and monoamine GPCRs (Figure 3D).

4. Discussion

4.1. Summary of principal findings

This study indicated the importance of ATX and LPA in the pathophysiology of HE, advocating them as potential biomarkers and therapeutic targets. The elevation of ATX levels was observed both in the liver parenchyma and frontal cortex of TAA-induced HE mice, indicating a systemic dysregulation associated with liver disease progression. Our previous findings also showed increased circulatory and cerebral levels of LPA in HE mice, while systemic inhibition of ATX attenuated these levels [19]. In another study using a mouse model of HE, inhibition of ATX decreased circulatory levels of LPA and its concentration in mice's hippocampus and cerebral cortex [28]. Moreover, in mouse models of advanced liver disease, plasma and liver ATX activity were increased [18]. We

Table 3. Correlation between serum ATX levels with laboratory parameters in cirrhotic-control and cirrhotic-HE groups.

Parameters	Serum ATX			
	Cirrhotic-Control		Cirrhotic-HE	
	Correlation coefficient (r)	P value	Correlation coefficient (r)	P value
Urea	**-0.62**	**0.04**	0.35	0.48
Creatinine	-0.44	0.17	0.31	0.49
Sodium	-0.52	0.09	-0.68	0.09
Potassium	-0.34	0.30	0.59	0.16
AST	0.35	0.28	-0.07	0.90
ALT	0.33	0.31	0.00	0.99
ALP	0.52	0.11	0.25	0.58
Total bilirubin	0.32	0.32	0.27	0.55
Direct bilirubin	0.23	0.48	0.33	0.46
WBC	0.20	0.55	0.48	0.27
RBC	-0.06	0.84	0.10	0.81
HB	0.19	0.55	0.46	0.28
HCT	0.16	0.62	0.32	0.47
MCV	0.31	0.34	0.65	0.11
MCH	0.24	0.46	**0.7**7	**0.04**
MCHC	0.01	0.97	0.65	0.11
PLT	**0.61**	**0.04**	-0.04	0.92
PMN	-0.46	0.15	0.64	0.13
Lymph	0.53	0.08	-0.58	0.17
PTT	-0.47	0.14	-0.02	0.95
INR	-0.36	0.26	0.19	0.67
Albumin	-0.39	0.23	-0.64	0.12
CRP	-0.61	0.08	0.00	0.98
MELD score	-0.54	0.08	0.52	0.22
MELD-Na score	-0.27	0.41	0.70	0.07
Child-Pugh Score	-0.23	0.54	0.63	0.12
West Haven Criteria	-	-	-0.14	-0.14

have previously demonstrated that ammonia also elevated the levels of LPA in astrocyte cultures [19]. It was also found in the present study that the serum levels of ATX are elevated in cirrhosis patients with HE relative to cirrhosis patients without HE. This highlights its potential role as a biomarker and suggests that the ATX-LPA axis represents a target of interest for therapeutic intervention. Previous studies have shown increased levels of ATX in patients with liver disease that were correlated with liver fibrosis scores [15, 16, 29-32].

4.2. ATX-LPA in HE: preclinical evidence

Our preclinical findings provide evidence of systemic and tissue-specific alterations in ATX during experimental HE. ATX concentrations were significantly elevated in both the liver parenchyma and frontal cortex of TAA-treated mice, indicating that alterations in the ATX system may extend beyond the diseased liver and involve the CNS. This observation is particularly relevant given the established contribution of neuroinflammatory and metabolic alterations to HE pathophysiology. Our previous study and study by Roy further demonstrated that circulating and cerebral LPA levels are increased in experimental HE and that pharmacological inhibition of ATX reduces LPA concentrations in the circulation, hippocampus, and cerebral cortex [19, 28]. Moreover, ammonia exposure increased LPA levels in cultured astrocytes [19], providing an additional link between a major HE-associated metabolic disturbance and ATX-LPA signaling.

The increased expression of Enpp2 in the salivary glands of HE mice also suggests that peripheral tissues may contribute to alterations in the ATX-LPA system during HE. Importantly, the present findings extend our previous observations by demonstrating change in ENPP2 gene expression at multiple sites relevant to the gut-liver-brain axis [19]. Previous studies have reported increased plasma and liver ATX activity in models of advanced liver disease and have shown that ATX inhibition can attenuate liver inflammation and fibrosis [18]. Collectively, these findings support the concept that ATX elevation may accompany the progression of liver dysfunction and may contribute to the biological environment associated with HE. Nevertheless, whether increased ATX is a driver of HE or primarily a consequence of advanced liver disease remains to be determined.

4.3. Clinical translation: ATX as a potential biomarker

The clinical findings provide translational support for the potential relevance of ATX in human HE. Both serum and salivary ATX concentrations were significantly higher in cirrhotic patients with HE than in cirrhotic patients without HE. These observations are consistent with previous

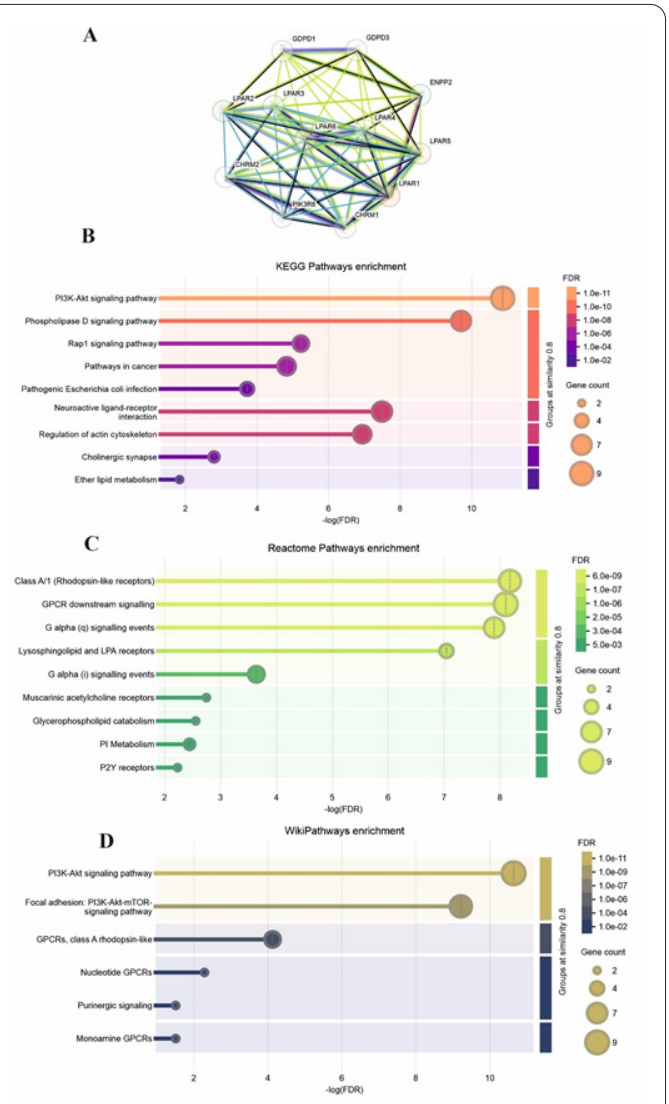


Fig. 3. Novel proteins and pathways associated with the ATX-LPA axis. (A) A network of the proteins related to the ATX-LPA axis, as determined by STRING. (B) KEGG pathways, (C) Reactome pathways, (D) and Wikipathways enrichment analysis for protein associated with ATX-LPA axis.

studies identifying circulating ATX as a marker of liver fibrosis, liver injury, and disease progression [15, 16, 29-32]. However, the present findings extend these observations by demonstrating an association between elevated ATX and the presence of HE in patients with cirrhosis. The positive correlation between salivary ATX and serum ALP in patients with HE further suggests that ATX may reflect the severity of underlying hepatic dysfunction. The detection of increased ATX in saliva is also of potential clinical interest because saliva collection is minimally invasive and may offer a practical approach for biomarker assessment. Nevertheless, these findings should be interpreted cautiously. Because ATX is also associated with hepatic fibrosis and other forms of chronic liver disease, its elevation may not be specific to HE itself. Larger and longitudinal studies are therefore required to determine whether ATX can discriminate HE from cirrhosis without HE, correlate with HE severity, or predict clinical outcomes. Combining ATX measurements with established clinical parameters and other HE-associated biomarkers may ultimately provide greater diagnostic or prognostic value than ATX alone.

4.4. Mechanistic implications of the ATX-LPA axis in HE

The biological relevance of ATX in HE may be related to its enzymatic generation of LPA, a bioactive lipid mediator that regulates diverse cellular processes through multiple LPA receptors [10-14]. Our findings are particularly relevant in light of previous experimental evidence showing that inhibition of ATX reduces hyperammonemia, systemic inflammation, and neuroinflammation and improves blood-brain barrier (BBB) integrity in experimental HE [19]. Similarly, inhibition of ATX has been reported to reduce LPA levels and neurological dysfunction in an acute HE model [28]. These observations suggest that increased ATX may contribute to HE not merely as a marker of liver disease but through modulation of downstream LPA-dependent signaling. Several mechanisms may potentially link ATX-LPA signaling to HE-associated hepatic and neurological alterations. LPA can activate hepatic stellate cells and promote inflammatory responses within the liver [32-34]. In the CNS, altered LPA signaling may influence astrocyte and other neural cell functions and contribute to neuroinflammatory responses. Our previous observation that ammonia increases LPA levels in astrocytes and that ATX inhibition reduces LPA and CCL3 levels in ammonia-exposed astrocyte cultures provides experimental support for a possible interaction between hyperammonemia and ATX-LPA signaling [19]. Thus, the ATX-LPA axis may represent one molecular link through which hepatic dysfunction and systemic metabolic disturbances contribute to neuroinflammation in HE.

The present findings also suggest that the effects of the ATX-LPA axis may involve broader inflammatory and intracellular signaling networks. The association of ATX-LPA-related proteins with PI3K-Akt and phospholipase D signaling pathways, as identified by our bioinformatics analysis, is consistent with the involvement of these pathways in cellular survival, inflammation, and signaling [35-37]. In addition, the association of LPA receptors with GPCR-dependent signaling provides a plausible framework for downstream effects of altered LPA availability. However, these mechanistic relationships remain to be experimentally established. Therefore, the current evidence supports the ATX-LPA axis as a biologically plausible contributor to HE pathophysiology, while further studies are required to determine the specific cellular targets and downstream pathways responsible for its effects.

4.5. Bioinformatics prediction of novel pathways

The identification of GDPD1 and GDPD3 is particularly intriguing, as these enzymes are involved in phospholipid metabolism and may modulate the availability of lysophosphatidylcholine, the substrate for ATX-mediated LPA production. This suggests a potential feedback or regulatory mechanism that could influence ATX activity. The muscarinic receptors CHRM1 and CHRM2 point to possible crosstalk between cholinergic signaling and LPA-mediated pathways, which is relevant given the known cholinergic dysfunction in cirrhosis and HE. PIK3R6 directly links the ATX-LPA axis to the PI3K-Akt signaling cascade. The pathway analyses indicated significant enrichment of signaling pathways, including PI3K/Akt and phospholipase D pathways, that influence cellular proliferation, survival,

and inflammation [35-37]. These pathways may directly relevant to HE pathogenesis, as they modulate neuroinflammation, BBB integrity, hepatic fibrogenesis, and neuronal signaling. The PI3K-Akt pathway, for instance, is a key regulator of liver regeneration and inflammatory responses [36], while phospholipase D has been implicated in neurodegenerative and neuroimmune diseases [37]. The identification of muscarinic receptors also raises the possibility that cholinergic dysfunction may intersect with LPA signaling, offering new therapeutic angles. However, these in silico predictions require experimental validation through knockdown/overexpression studies or pharmacological inhibition.

4.6. Limitations

Several limitations should be considered for this study. First, the relatively small number of cirrhotic patients limits the statistical power of the clinical analyses and the generalizability of the observed associations. Larger, multicenter cohorts will be necessary to validate the association between ATX and HE and to establish its diagnostic and prognostic value. Second, the clinical component of the study provides observational evidence of an association between ATX levels and HE but does not establish causality. In particular, the elevation of ATX may reflect the severity of underlying liver disease rather than being specific to the development of HE. Longitudinal studies incorporating patients before, during, and after episodes of HE will therefore be important to determine whether ATX changes dynamically with neurological deterioration and recovery. Third, although the TAA-induced mouse model provides a useful experimental platform for investigating HE-associated hepatic and neurological alterations, no animal model fully reproduces the complex pathophysiology of human HE. Differences between experimental and human disease may limit the direct translation of the present findings to clinical settings. Fourth, the bioinformatics analysis was primarily hypothesis-generating and was based on predicted protein-protein interactions and pathway enrichment. The newly identified proteins and signaling pathways, including GDPD1, GDPD3, CHRM1, CHRM2, PIK3R6, and the PI3K-Akt and phospholipase D pathways, require experimental validation before their direct involvement in ATX-LPA-mediated HE can be established. Finally, although ATX was evaluated in multiple biological compartments, the cellular and molecular mechanisms responsible for its elevation and its contribution to neuroinflammation remain incompletely defined. Future studies using cell-specific approaches, longitudinal clinical designs, and targeted mechanistic experiments are warranted to address these limitations.

5. Conclusion

This study provides compelling evidence for the involvement of the ATX-LPA axis in HE pathophysiology. The consistent elevation of ATX across experimental and clinical settings, in liver tissue, cerebral cortex, serum, and saliva, supports its role as a potential biomarker and therapeutic target. The correlation between salivary ATX and serum ALP suggests non-invasive monitoring may be feasible. While these findings are promising, several questions remain: the precise mechanisms by which ATX contributes to neuroinflammation in HE, the relative contribution of peripheral versus central ATX sources, and the utility of ATX-targeted therapies in clinical settings. Future investigations should explore the therapeutic potential of existing LPAR antagonists and ATX inhibitors, and evaluate the diagnostic performance of salivary ATX in larger prospective cohorts. By bridging preclinical models with clinical observations, our work lays a foundation for translating ATX-LPA axis modulation into clinical practice for HE patients.

Conflict of Interests

The author has no conflicts with any step of the article preparation.

Consent for publications

The author read and approved the final manuscript for publication.

Ethics approval and consent to participate

All experimental animal procedures were conducted following ARRIVE guidelines and were approved by the Ethical Committee of Animal Care at Iran University of Medical Sciences, Tehran, Iran (IR.IUMS.REC.1398.959). The clinical section of the study received approval from the Institutional Review Board Ethics Committee of Mashhad University of Medical Sciences, Mashhad, Iran (IR.MUMS.MEDICAL.REC.1401.141), and the protocol conforms to the provisions of the Declaration of Helsinki.

Informed Consent

Informed consent was obtained from all patients or their legal guardians.

Availability of data and material

The data that support the findings of this study are available from the corresponding author upon reasonable request.

Authors' contributions

A.S: Writing an original draft, methodology, data curation, visualization, investigation and editing; H.Z: Writing original draft, data curation; F.M: Writing original draft, data curation; S.S: Data curation; M.H.A: Writing original draft; F.R: Data curation; M.M: Data curation; V.H: Data curation; A.B.N, S.S.N, and A.SH: Writing original draft, project administration, supervision, review and editing.

Funding

This study was supported by a grant from Mashhad University of Medical Sciences, Mashhad, Iran (Grant No. 4001099).

Availability of data and materials

All data generated or analyzed during this study are included in this manuscript or available from the corresponding authors upon reasonable request.

References

1. Hurtado-Díaz-de-León I, Tapper EB (2025) Systems of care that improve outcomes for people with hepatic encephalopathy. Metab Brain Dis 40(1): 1–11 doi: 10.1007/s11011-024-01430-8
2. He X, et al. (2025) The gut–brain axis underlying hepatic encephalopathy in liver cirrhosis. Nat Med 2025: 1–12 doi: 10.1038/s41591-024-03405-9
3. Gallego JJ, et al. (2025) Ammonia and beyond – biomarkers of

hepatic encephalopathy. Metab Brain Dis 40(1): 100 doi: 10.1007/s11011-024-01512-7
4. Sepehrinezhad A, et al. (2024) Correlation of ammonia and blood laboratory parameters with hepatic encephalopathy: A systematic review and meta-analysis. PLoS One 19(9): e0307899 doi: 10.1371/journal.pone.0307899
5. Fujimori N, et al. (2018) Serum autotaxin levels are correlated with hepatic fibrosis and ballooning in patients with non-alcoholic fatty liver disease. World J Gastroenterol 24(11): 1239–1249 doi: 10.3748/wjg.v24.i11.1239
6. Iwadare T, et al. (2024) Serum autotaxin is a prognostic indicator of liver-related events in patients with non-alcoholic fatty liver disease. Commun Med 4(1): 73 doi: 10.1038/s43856-024-00499-7
7. Shao X, et al. (2020) Usefulness of autotaxin for the complications of liver cirrhosis. World J Gastroenterol 26(1): 97–108 doi: 10.3748/wjg.v26.i1.97
8. Qiu H, et al. (2022) Hepatocyte-Secreted Autotaxin Exacerbates Nonalcoholic Fatty Liver Disease Through Autocrine Inhibition of the PPARα/FGF21 Axis. Cell Mol Gastroenterol Hepatol 14(5): 1003–1023 doi: 10.1016/j.jcmgh.2022.07.012
9. Nie C, et al. (2020) Autotaxin: An Early Warning Biomarker for Acute-on-chronic Liver Failure. J Clin Transl Hepatol 8(3): 240–245 doi: 10.14218/JCTH.2020.00045
10. Okudaira S, Yukiura H, Aoki J (2010) Biological roles of lysophosphatidic acid signaling through its production by autotaxin. Biochimie 92(6): 698–706 doi: 10.1016/j.biochi.2010.04.015
11. Valdés-Rives SA, González-Arenas A (2017) Autotaxin-Lysophosphatidic Acid: From Inflammation to Cancer Development. Mediators Inflamm 2017(1): 9173090 doi: 10.1155/2017/9173090
12. Geraldo LHM, et al. (2021) Role of lysophosphatidic acid and its receptors in health and disease: novel therapeutic strategies. Signal Transduct Target Ther 6(1): 45 doi: 10.1038/s41392-020-00367-5
13. Lin M-E, Herr DR, Chun J (2010) Lysophosphatidic acid (LPA) receptors: Signaling properties and disease relevance. Prostaglandins Other Lipid Mediat 91(3): 130–138 doi: 10.1016/j.prostaglandins.2009.02.002
14. Noguchi K, et al. (2009) Lysophosphatidic acid (LPA) and its receptors. Curr Opin Pharmacol 9(1): 15–23 doi: 10.1016/j.coph.2008.11.010
15. Joshita S, et al. (2018) Serum autotaxin is a useful liver fibrosis marker in patients with chronic hepatitis B virus infection. Hepatol Res 48(4): 275–285 doi: 10.1111/hepr.12997
16. Wunsch E, et al. (2016) Serum Autotaxin is a Marker of the Severity of Liver Injury and Overall Survival in Patients with Cholestatic Liver Diseases. Sci Rep 6(1): 30847 doi: 10.1038/srep30847
17. Booijink R, et al. (2022) A type IV Autotaxin inhibitor ameliorates acute liver injury and nonalcoholic steatohepatitis. EMBO Mol Med 14(9): e16333 doi: 10.15252/emmm.202216333
18. Bain G, et al. (2017) Selective Inhibition of Autotaxin Is Efficacious in Mouse Models of Liver Fibrosis. J Pharmacol Exp Ther 360(1): 1–13 doi: 10.1124/jpet.116.237156
19. Sepehrinezhad A, et al. (2023) Inhibition of autotaxin alleviates pathological features of hepatic encephalopathy at the level of gut–liver–brain axis: an experimental and bioinformatic study. Cell Death Dis 14(8): 490 doi: 10.1038/s41419-023-06022-5
20. Butterworth RF (2021) Ammonia Removal by Metabolic Scavengers for the Prevention and Treatment of Hepatic Encephalopathy in Cirrhosis. Drugs R D 21(2): 123–132 doi: 10.1007/s40268-021-00345-4
21. Vilstrup H, et al. (2024) Down the road towards hepatic encephalopathy. Urea synthesis - the liver workhorse of nitrogen metabolism. Metab Brain Dis 40(1): 49 doi: 10.1007/s11011-024-01437-1
22. Katayama K, Kakita N (2024) Possible pathogenetic role of ammonia in liver cirrhosis without hyperammonemia of venous blood: The so-called latency period of abnormal ammonia metabolism. Hepatol Res 54(3): 235–243 doi: 10.1111/hepr.14022
23. Sepehrinezhad A, et al. (2021) Drug-induced-acute liver failure: A critical appraisal of the thioacetamide model for the study of hepatic encephalopathy. Toxicol Rep 8: 962–970 doi: 10.1016/j.toxrep.2021.04.011
24. Durand F, Valla D (2005) Assessment of the prognosis of cirrhosis: Child-Pugh versus MELD. J Hepatol 42(1): S100–S107 doi: 10.1016/j.jhep.2004.11.015
25. Tsoris A, Marlar CA (2025) Use Of The Child Pugh Score In Liver Disease. StatPearls. Treasure Island (FL): StatPearls Publishing
26. Botta F, et al. (2003) MELD scoring system is useful for predicting prognosis in patients with liver cirrhosis and is correlated with residual liver function: a European study. Gut 52(1): 134–139 doi: 10.1136/gut.52.1.134
27. Montagnese S, et al. (2022) EASL Clinical Practice Guidelines on the management of hepatic encephalopathy. J Hepatol 77(3): 807–824 doi: 10.1016/j.jhep.2022.06.001
28. Roy S, et al. (2022) Inhibition of Autotaxin Ameliorates LPA-Mediated Neuroinflammation and Alleviates Neurological Dysfunction in Acute Hepatic Encephalopathy. ACS Chem Neurosci 13(19): 2829–2841 doi: 10.1021/acschemneuro.2c00046
29. Nakagawa H, et al. (2011) Autotaxin as a novel serum marker of liver fibrosis. Clin Chim Acta 412(13-14): 1201–1206 doi: 10.1016/j.cca.2011.03.014
30. Joshita S, et al. (2018) Serum Autotaxin Is a Useful Disease Progression Marker in Patients with Primary Biliary Cholangitis. Sci Rep 8(1): 8159 doi: 10.1038/s41598-018-26531-0
31. Honda Y, et al. (2019) Autotaxin is a valuable biomarker for the prediction of liver fibrosis in patients with non-alcoholic fatty liver disease. Hepatol Res 49(10): 1136–1146 doi: 10.1111/hepr.13382
32. Kaffe E, et al. (2017) Hepatocyte autotaxin expression promotes liver fibrosis and cancer. Hepatology 65(4): 1369–1383 doi: 10.1002/hep.28973
33. Coulouarn C, Clément B (2014) Stellate cells and the development of liver cancer: therapeutic potential of targeting the stroma. J Hepatol 60(6): 1306–1309 doi: 10.1016/j.jhep.2014.02.003
34. Fujita T, Narumiya S (2016) Roles of hepatic stellate cells in liver inflammation: a new perspective. Inflamm Regen 36: 1 doi: 10.1186/s41232-016-0005-6
35. Shamsan E, et al. (2024) The role of PI3k/AKT signaling pathway in attenuating liver fibrosis: a comprehensive review. Front Med (Lausanne) 11: 1389329 doi: 10.3389/fmed.2024.1389329
36. Zhang C, et al. (2024) Signaling pathways of liver regeneration: Biological mechanisms and implications. iScience 27(1): 108683 doi: 10.1016/j.isci.2023.108683
37. Zhang W, et al. (2024) Phospholipase D, a Novel Therapeutic Target Contributes to the Pathogenesis of Neurodegenerative and Neuroimmune Diseases. Anal Cell Pathol 2024(1): 6681911 doi: 10.1155/2024/6681911